Catalysis Today 169 (2011) 192–199

Contents lists available at ScienceDirect

Catalysis Today

journal homepage: www.elsevier.com/locate/cattod

# The effect of oxygen adsorption on catalytic activity of $SnO_2$ in CO oxidation

Ireneusz Kocemba*, Jacek M. Rynkowski

*Institute of General and Ecological Chemistry, Technical University of Łódź, 90-924 Łódź, Żeromskiego 36, Poland*

ARTICLE INFO

*Article history:*
Available online 25 October 2010

*Keywords:*
Tin dioxide
Carbon monoxide oxidation
Oxygen TPD
TPR-CO

ABSTRACT

A sequence of thermal treatments in oxygen was undertaken to study the influences of oxygen adsorption on the catalytic activity of $SnO_2$ in CO oxidation. Commercial $SnO_2$ (Fluka) and tin dioxide obtained from $SnCl_4$ were characterized using XTD, BET, SEM TPD, and TPR methods. Catalytic activity of $SnO_2$ samples was carried out as a function of pre-treatment temperature in oxygen. Due to the presence of different reactive oxygen forms, CO oxidation shows the hysteretic course. The approach to the differentiated mechanism of CO oxidation over $SnO_2$ has been presented. The results obtained should be useful in understanding how the oxygen adsorption affects the catalytic activity of tin dioxide towards CO oxidation.



## 1. Introduction

The catalytic low temperature oxidation of carbon monoxide has been studied on numerous both metallic and oxide catalysts over the years. This reaction is of great practical importance due to its relevance in applications such as air purification, pollution control devices, closed-cycle $CO_2$ lasers, cleanup automobile emissions during cold start etc.

$SnO_2$ is a reducible oxide (n-type semiconductor) with a wide band gap (3.6 eV) and rutile bulk structure [1]. It is one of the most widely used semiconductor oxides for the manufacturing of sensors used for monitoring the environment [2–5]. Tin dioxide may also be applied as a catalyst, catalyst support [6], an interesting material for chemically resistant electrode [7] or an optoelectronic device [8].

Although the catalytic activity of pure $SnO_2$ in the oxidation reactions is rather poor, tin dioxide has been intensively studied as a support for noble metal catalysts during the last two decades [9,10]. $Pt/SnO_2$ was reported as an active catalyst in reactions of low temperature CO or $CH_4$ oxidation [11,12]. Grass and Lintz [13] suggested a probable pathway of CO oxidation over $Pt/SnO_2$ catalyst, which assumed an adsorption of oxygen on $SnO_2$ followed by its migration to the reaction sites situated at the border between oxide and platinum metal particles. Therefore the capacity of $SnO_2$ for $O_2$ adsorption seems to be very important because of its participation in the total catalytic activity of the $Pt/SnO_2$ systems in CO oxidation.

Platinized tin oxide shows high activity and selectivity in oxidation of carbon monoxide in the presence of hydrogen (PROX—preferential oxidation). One can anticipate that also in this case catalytic efficiency of $Pt/SnO_2$ catalysts is connected with $O_2$ adsorption [14].

Yamaguchi et al. [15] have investigated methane oxidation on the reduced $SnO_2$ surface. Their results reveal that $O^-$ species adsorbed on the $SnO_2$ surface are the main active centre for the dissociation of C–H bond in methane.

Chemisorption of oxygen by $SnO_2$ is also crucial for the mechanism of gas detection occurring on resistive semiconductor gas sensors. Such a mechanism is connected with oxygen chemisorption followed by catalytic oxidation of the detected gas [16]. For instance, a simple reaction scheme describing the process of carbon monoxide detection can be written as:

$$O_2 + 2e \rightarrow 2O^- \quad (1)$$

$$CO + O^- \rightarrow CO_2 + e \quad (2)$$

Therefore from the catalytic point of view, the gas detection properties depend mainly on the ability to oxygen adsorption.

Several different instrumental methods e.g. FTIR (Fourier transformed infrared), TPD (temperature-programmed desorption), EPR (electron paramagnetic resonance), etc. were used to characterize various oxygen species chemisorbed on $SnO_2$ surface. On the basis of these measurements [17–19] it was proposed that adsorbed oxygen turns into various oxygen species transferring an electron from $SnO_2$ to the chemisorbed oxygen according to the following processes:

$$O_2(gas) \Leftrightarrow O_2(ad) \Leftrightarrow O_2^- \Leftrightarrow O^-(ad) \Leftrightarrow O^{2-}(ad) \Leftrightarrow O^{2-}(lattice) \quad (3)$$

Adsorbed oxygen species are involved in different catalytic oxidation reactions. Their nature depends on the temperature. Below

* Corresponding author. Tel.: +48 42 631 31 34; fax: +4842 6313128.
*E-mail address:* ikocemba@p.lodz.pl (I. Kocemba).

0920-5861/$ – see front matter © 2010 Elsevier B.V. All rights reserved.
doi:10.1016/j.cattod.2010.09.015

180 °C oxygen adsorption occurs in a form of $O_2^-$, while above this temperature to ca. 350 °C the $O^-$ form predominates. Over 30 years ago Bielański and Haber [18] classified the metal oxides into three main groups (p-type semiconducting oxides, n-type semiconductors and binary oxides) depending on their interaction with $O_2$. They claimed that for n-type semiconductors $O_2^-$ and $O^-$ forms predominate. Che and Tench in their fundamental reviews [19] proved, that the wide range of oxygen species can be observed on all these metal oxides given the right conditions although their thermal stability varies considerably.

It is obvious that adsorption properties of tin dioxide depend on the surface structure and therefore on the methods of $SnO_2$ preparation. $SnO_2$ has been widely fabricated using a variety of techniques. Those methods were described in detail in works [20–22].

In this paper the influence of oxygen chemisorption on the catalytic activity of differently prepared $SnO_2$ samples in CO oxidation was studied. In spite of many experimental and theoretical works describing the mechanism of oxygen adsorption on $SnO_2$ surface, the effect of this process on $SnO_2$ catalytic activity is still ambiguous.

## 2. Experimental

### 2.1. Sample preparation

The tin chloride ($SnCl_4{\cdot}5H_2O$, analytical grade) and ammonia ($NH_3{\cdot}H_2O$, analytical grade) were used as raw materials. The $SnCl_4{\cdot}5H_2O$ was dissolved in distilled water to form transparent solution. An aqueous solution of $SnCl_4$ was hydrolysed with an ammonia solution

$$SnCl_4 + 4NH_4OH \Rightarrow SnO_2{\cdot}nH_2O + 4NH_4Cl + (2-n)H_2O \quad n \leq 2 \quad (4)$$

The obtained white precipitates were washed with distilled water for several times, dried at 120 °C for 16 h and finally calcined at 600 °C in air for 4 h. The sample was denoted as $SnO_2$(Cl).

The properties of $SnO_2$(Cl) powders were compared to the commercial $SnO_2$ (Fluka 96550), which was denoted as $SnO_2$(Fl).

### 2.2. Structural and morphological characterization of samples

Specific surface area of $SnO_2$ was determined by BET method using a Carlo Erba Sorptomatic 1900 apparatus.

X-ray diffraction (XRD) patterns were obtained at room temperature using a PANalytical X'Pert Pro MPD diffractometer operating at 40 kV and 30 mA (CuKα radiation) Data were collected in the range of $2\theta = 0–80°$ with a step size of 0.0167° and step time of 10 s. JCPDS-ICDD files were used for phase identification.

The particle morphology of samples was investigated by scanning electron microscopy with energy dispersive X-ray spectroscopy (SEM-EDS) using a S-4700 Hitachi system.

Differential thermal analysis (DTA) and thermogravimetric analysis (TGA) were carried out in the atmosphere of air (Setsys 16/18, Setaram).

### 2.3. Oxygen adsorption

Oxygen adsorption was measured using temperature-programmed desorption method ($O_2$-TPD) with an application of a zirconium oxygen analyser (Z110, Hitech Instruments Ltd., Luton, England). This device shows very high sensitivity (oxygen detection limit 0.1 ppm) and is highly selective to oxygen. Prior to oxygen adsorption, the sample of 0.2 g was *in situ* pre-treated by heating in ultra pure (99.9999%) Ar flow for 1 h at a temperature 600 °C, followed by cooling to room temperature. Next, argon was replaced by oxygen, which was passing through the reactor with a flow rate of 40 $cm^3\ min^{-1}$ at different temperatures in the range 25–800 °C for 1 h. One can assume that after such treatment the samples were free from hydroxyl groups [23].

After cooling to room temperature, oxygen flow was replaced by argon and the temperature-programmed desorption of oxygen was recorded in the temperature range 25–800 °C at a heating rate of 20 °/min.

### 2.4. TPR measurements

Temperature-programmed reduction (TPR-CO) measurements were carried out in PEAK-4 apparatus [24], using CO as a reducing agent. TPR-CO experiments were performed using CO/Ar (5 vol.% CO, 95 vol.% Ar) gas mixture, with a flow rate of 40 $cm^3\ min^{-1}$, in the temperature range 25–760 °C with a linear ramp rate of 15 °C $min^{-1}$. Prior to the TPR run, the sample of 0.2 g was *in situ* pre-treated by heating in either $O_2$ or Ar flow for 1 h at a given temperature in the range 25–760 °C, followed by cooling to room temperature. The presence of $CO_2$ in the effluent gas due to the reduction of the sample was monitored by the $CO_2$ infrared gas analyser (Fuji Electric System Co., type ZRJ-4).

### 2.5. Catalytic test

Temperature-Programmed Surface Reaction (TPSR) method was used to measure catalytic activity in the temperature range 25–760 °C. The mass of the sample of 0.2 g, the stream of the reacting gases CO/air (0.35 vol.% CO, 99.65 vol.% air) or (0.72 vol.% CO, 99.28 vol.% air) and a linear increase and decrease in temperature (5 °/min) were used. Behind the reactor, the concentration of $CO_2$ was constantly measured by the $CO_2$ infrared gas analyser (Fuji Electric System Co., type ZRJ-4).

Prior to oxidation, the samples were heated in $O_2$ stream at a given temperature within the range 200–760 °C for 1 h.

The adjustment and monitoring of the total gas flow, temperature and $CO_2$ concentration behind the reactor were controlled by computer.

The catalytic activity was expressed as the temperature of 50% CO conversion reached during an increase ($T_{50i}$) and decrease ($T_{50d}$) in the temperature. The difference ($T_{50i} - -T_{50d}$) reflecting hysteretic changes of catalytic activity was denoted as $\Delta T_H$.

## 3. Results

### 3.1. Characterization of the samples

Fig. 1 shows thermo gravimetric and differential thermal analysis patterns of $SnO_2$(Cl) sample before its calcination. Two steps of weight loss can be observed on TG curve the massive at 100 °C and smaller at 220–550 °C, which can be attributed to the removal of physical and chemisorbed water, respectively.

The masses of both samples investigated stabilize at above 550 °C. That is why the temperature of 600 °C was chosen as a final temperature of samples calcination.

The X-ray diffraction patterns of $SnO_2$ samples are shown in Fig. 2. The calcined samples correspond to the cassiterite phase. $SnO_2$(Cl) powders show the same diffraction lines as the commercial $SnO_2$(Fl) and their intensity is very similar.

The average crystallite size of $SnO_2$ was determined basing on Scherrer equation taking into consideration the broadening of [1 1 0] diffraction line [25]. The calculated values are presented in Table 1. The crystallite size of both investigated $SnO_2$ samples is almost the same.

The BET surface area of the samples under study is reported in Table 1. The $SnO_2$(Cl) sample shows a higher surface area than

**Table 1**
Properties of $SnO_2$ samples.

| Sample code | Mean crystallite size (calculated from XRD) [nm] | BET surface are [$m^2$/g] | Particle diameter (calculated from SEM) [nm] | BET surface are[a] [$m^2$/g] |
|---|---|---|---|---|
| $SnO_2$(Cl) | 109 | 8.2 | 300 | 7.6 |
| $SnO_2$(Fl) | 113 | 6.2 | 300 | 6.2 |

[a] After heating at 800 °C in oxygen.

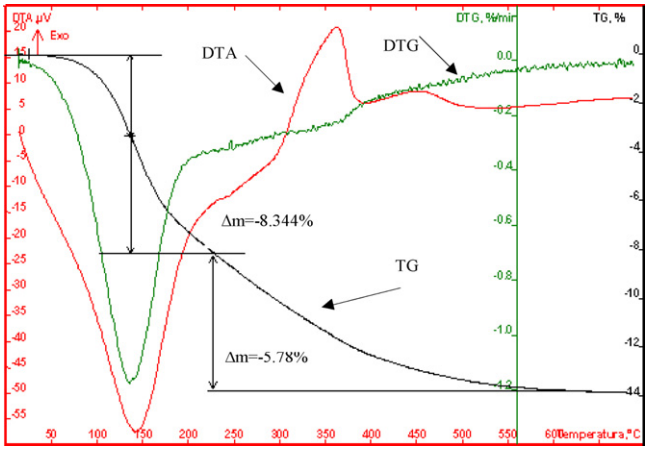


**Fig. 1.** Thermal analysis of $SnO_2$(Cl) sample precursor.

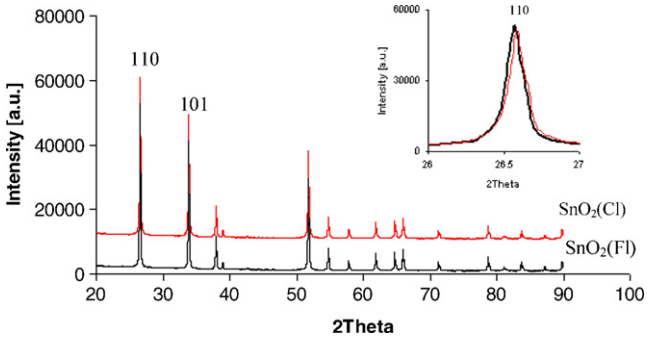


**Fig. 2.** XRD patterns of $SnO_2$ samples.

$SnO_2$(Fl). To get a better insight into the morphology of $SnO_2$ SEM photographs were taken (Fig. 3). The pictures of both $SnO_2$ samples are similar. The comparison of two magnifications ×900 and ×15,000 of the sample $SnO_2$(Cl) reveals large agglomerates ca. 10–15 μm (Fig. 3a), which consist of small (≈0.3 μm) spherical particles of $SnO_2$ (Fig. 3b). The structure of $SnO_2$(Fl) is in fact identical (Fig. 3c).

### 3.2. Oxygen adsorption

The TPD-$O_2$ profiles of the investigated samples are presented in Fig. 4a and b. It can be observed that the area of recorded peaks strongly increases with an increase in the adsorption temperature. The adsorption at room temperature results in a very small desorption peak at ca. 150 °C.

The oxygen desorption from both samples after their heating in oxygen at temperatures higher than 200 °C occurs in two stages. The maximum of desorption for the first peak occurs at ca. 650 °C and for the second at over 800 °C.

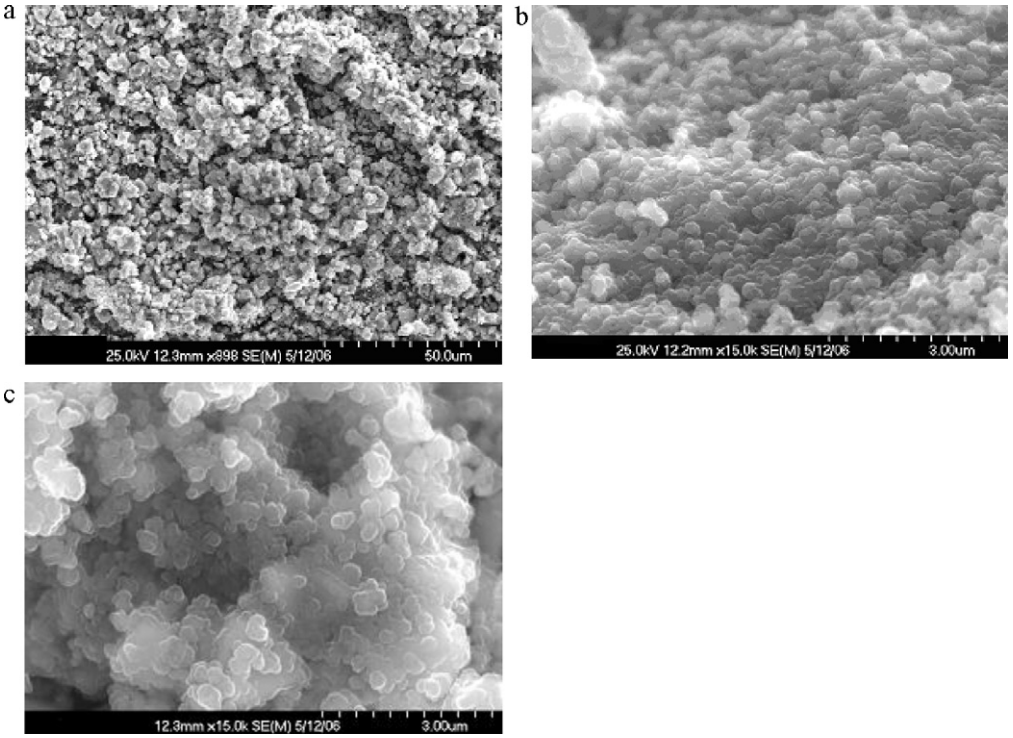


**Fig. 3.** SEM pictures of the surface of $SnO_2$ samples. Magnifications ×900 (a), ×15,000 (b) $SnO_2$(Cl) and ×15,000 (c) $SnO_2$(Fl).

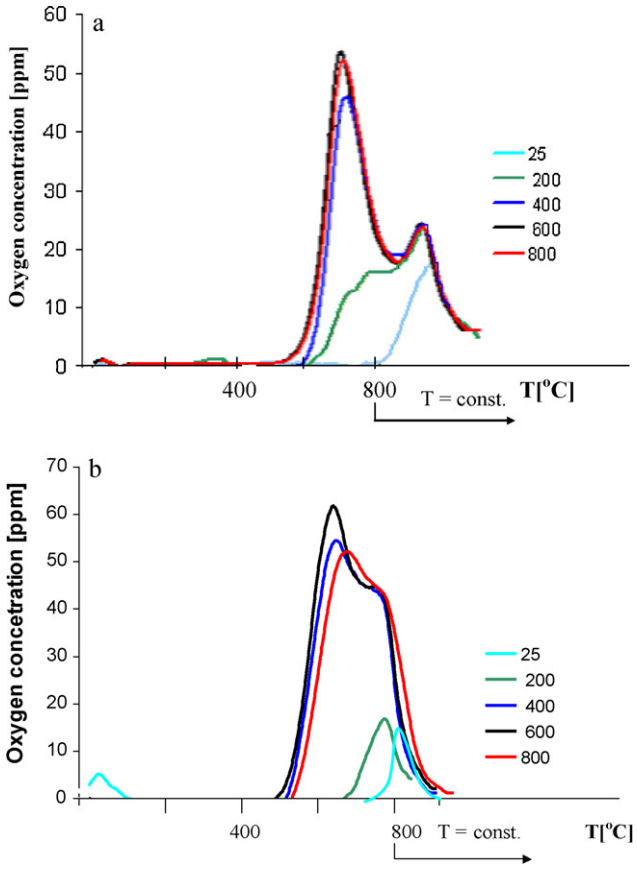


**Fig. 4.** (a) TPD-$O_2$ profiles of $SnO_2$(Fl) sample after pre-treatment in oxygen at different temperature [°C]. (b) TPD-$O_2$ profiles of $SnO_2$(Cl) sample after pre-treatment in oxygen at different temperature [°C].

TPD-$O_2$ studies over $SnO_2$ oxide have been reported in a few works [26,27]. The general conclusion is that the course of TPD strongly depends on the pre-treatment of the catalyst surface preceding the desorption process.

$SnO_2$ is a berthollide type, unstoichiometric compound, which shows a deficiency of $O^{2-}$ ions towards $Sn^{4+}$. Thus, the predominant adsorptive centres are oxygen vacancies, which can be formed on the $SnO_2$ surface both during the preparation and the temperature pre-treatment of the sample in an appropriate atmosphere. In general, the heating in oxygen leads to the decrease of their concentration whereas in a reductive or neutral atmosphere to the increase. Thus the adsorption of oxygen may be considered as the process of oxidation of $SnO_2$ surface whereas the desorption of oxygen as reduction. The efficiency of these processes for the particular $SnO_2$ sample depends on the temperature.

Yamazoe et al. [28] reported desorption of four kinds of different oxygen species: $O_2$ at 80 °C, $O_2^-$ at 150 °C, $O^-$ (or $O^{2-}$) at 450–600 °C and lattice oxygen above 600 °C. Following these findings we could attribute our TPD peaks to particular oxygen species: The peaks which arise at the lowest temperatures (<200 °C) denoted as A, were ascribed to $O_2$, or $O_2^-$ while those which arise at ca. 600 °C, denoted as B, to $O^-$. The peaks which arise at the highest temperatures were denoted as L and attributed to the removal of lattice oxygen $O^{2-}$.

To summarize, two forms of oxygen, namely B ($O^-$) and lattice oxygen L ($O^{2-}$), were observed after $SnO_2$ heating in oxygen at temperatures higher than 200 °C, while $SnO_2$ sample heated in oxygen at temperatures lower than 200 °C showed practically only the L ($O^{-2}$) form. Thus it can be assumed that B peaks describe real properties of $SnO_2$ as an oxygen adsorbent.

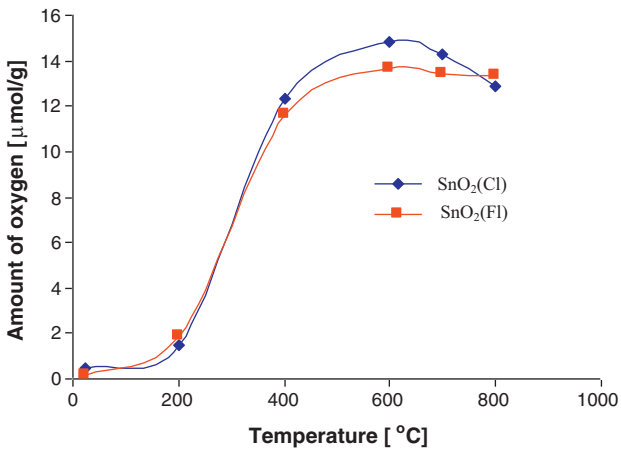


**Fig. 5.** Dependence of the amount of desorbed $O_2$ vs. temperature of $O_2$ adsorption.

Fig. 5 shows the amount of desorbed oxygen calculated from the area under the TPD curves vs. temperature of oxygen adsorption. Both samples show similar adsorption. The amount of oxygen adsorbed on $SnO_2$(Fl) sample gets stable from ca. 500 °C. For the sample $SnO_2$(Cl) the slight decrease of the amount of adsorbed oxygen is observed at the temperatures 700 and 800 °C, connected with the small escape of BET surface (Table 1) of this sample, as a result of its heating at the temperatures higher than calcination temperature.

An influence of time on the amount of adsorbed oxygen at 600 °C was checked in an additional experiment. The TPD profiles after heating for 5, 10, 20, 40 and 80 min, respectively, were, in fact identical.

### 3.3. TPR-CO measurements

Fig. 6 shows the TPR-CO profile of $SnO_2$(Fl) sample after heating in argon at 600 °C for 1 h (black curve). One can observe an evolution of $CO_2$ in the temperature range 270–500 °C with the maximum at ca. 350 °C, which can be attributed to the surface reduction of $SnO_2$ described by the equation:

$$(SnO_2)_s + CO = (SnO)_s + CO_2 \quad (5)$$

At the temperature of 600 °C, a rapid increase in $CO_2$ evolution reflecting the start of bulk reduction of $SnO_2$ is clearly seen. TPR-CO profiles of $SnO_2$(Cl–)—not shown here—are in fact identical.

The TPR-CO profiles of the samples pre-treated in oxygen at the temperatures in the range 25–500 °C, are in fact similar to those heated just in argon. The blue, green and red TPR profiles in Fig. 6 were obtained after heating the $SnO_2$(Fl) sample in oxygen for 1 h at 600, 700 and 760 °C, respectively. The new low temperature reduc-

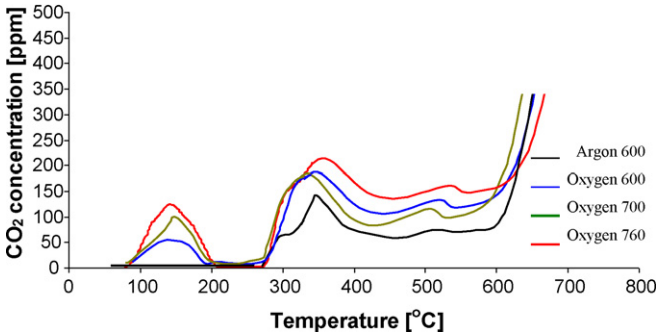


**Fig. 6.** TPR-CO profiles of $SnO_2$(Fl) sample pre-treated in argon or oxygen at different temperatures [°C].

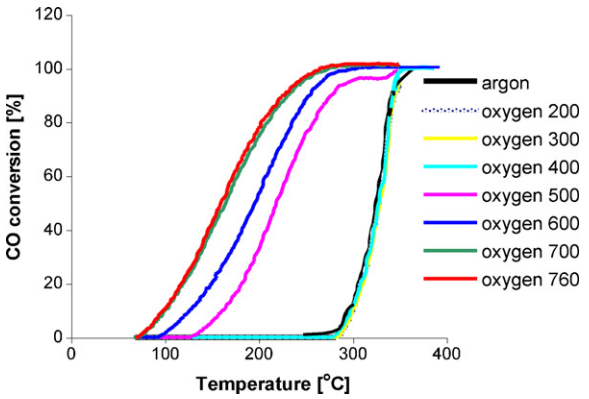


**Fig. 7.** CO conversion as a function of temperature for $SnO_2$(Fl) sample pre-treated in argon or oxygen at different temperatures [°C].

tion range (100–200 °C, maximum at ca. 150 °C) is now observed. The intensity of these peaks, connected with the removal of oxygen adsorbed at the temperature ≥600 °C, significantly increases with the increase in the oxygen pre-treatment temperature. As we have earlier shown in Fig. 5, the amount of oxygen desorbing from SnO2(Fl) sample after its pre-treatment in oxygen at the temperature >500 °C is practically stable. Thus one could expect that the intensity of low temperature peaks on TPR-CO profiles, should be also similar. However it is not. Such a discrepancy may suggest that on the total amount of desorbed oxygen presented in Fig. 5 contribute two forms of adsorbed oxygen: "inactive" and "active". If so the low temperature TPR peak may be attributed to the removal of "active" adsorbed oxygen form.

### 3.4. Catalytic test

Fig. 7 shows the conversion of CO as a function of temperature for $SnO_2$(Fl) sample pre-treated in argon or oxygen at different temperatures. The catalytic activity of the sample, heated in oxygen at the temperature up to 400 °C is identical to that pre-treated in argon. Only heating in oxygen at the temperature ≥500 °C leads to a very significant increase in catalytic activity. The optimum activity is reached after the activation in oxygen at the temperature ≥700 °C. Thus one can claim that the temperature of pre-treatment and quantity of oxygen adsorbed influence the catalytic activity of $SnO_2$.

The hysteresis of the catalytical activity is observed when we record the changes of conversion during an increase and subsequent decrease in the temperature (Fig. 8). This process is presented for the $SnO_2$(Fl) sample pre-treated in oxygen at 760 °C (red curves) and at 200 °C (black curves). The hysteretic change of catalytic activity $\Delta T_H = T_{50i} - -T_{50d}$ can be either positive (+) or negative (−), depending on the temperature of pre-treatment in oxygen. $\Delta T_H$ values for the discussed samples are −−95 °C and +35 °C, respectively. Table 2 presents the calculated values of $T_{50}$ and $\Delta T_H$ showing the similar behaviour of both the investigated samples.

It is interesting to compare the results of CO conversion in the first and second TPRS run. The samples pre-treated in oxygen at

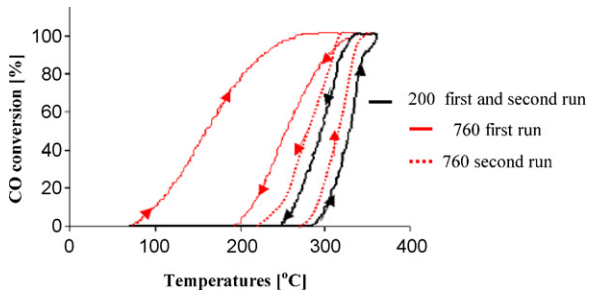


**Fig. 8.** CO conversion in the first and second TPRS run for $SnO_2$(Fl) sample pre-treated in oxygen at different temperatures [°C].

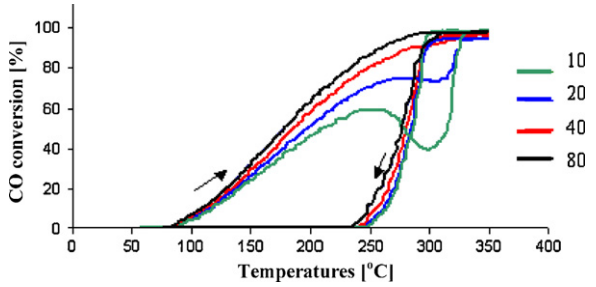


**Fig. 9.** CO conversion vs. temperature after heating the $SnO_2$(Fl) sample in oxygen at 600 °C for 10, 20, 40 and 80 min.

temperatures up to 400 °C show that the second TPSR run is identical as the first one. However, when the sample is pre-treated in oxygen at the temperature ≥500 °C the second TPSR run strongly changes in comparison with the first one. In Fig. 8 the dashed red line of hysteresis curve represents the second run. The catalytic activity significantly decreases and $\Delta T_H$ value shows a reverse sign. It seems to indicate that during the first run adsorbed oxygen is completely removed from the $SnO_2$ surface and that during CO oxidation the rate of oxygen readsorption is very low.

As it has already been mentioned, the results presented above indicate that the catalytic activity of $SnO_2$ in the reaction of CO oxidation strongly depends on its pre-treatment in oxygen atmosphere.

Fig. 9 depicts the changes in CO conversion vs. temperature after heating the $SnO_2$(Fl) sample in oxygen at 600 °C for 10, 20, 40 and 80 min. The conversion starts at the same temperature (ca. 80 °C), but the shape of TPSR profile depends on the time of heating. This shape suggests that the concentration of oxygen increases with the heating time. Such a conclusion is inconsistent with the $O_2$--TPD results presented earlier, which indicated no correlation between the time of $O_2$ adsorption and the amount of $O_2$ adsorbed.

To explain this discrepancy we assumed that the time of pre-treating in oxygen increases only the surface concentration of oxygen showing high reactivity. It results a higher activity is observed when $SnO_2$ samples were heated at high temperatures ≥500 °C. It also causes different values of $\Delta T_H$ parameter depending on the adsorption temperature, The sequence of several successive processes of CO oxidation in the temperature range 400–700 °C

**Table 2**
Influence of the temperature of heating in oxygen on the catalytic activity of $SnO_2$.[a]

| Temperature of heating in oxygen | 300 [°C] | | | 400 [°C] | | | 500 [°C] | | | 600 [°C] | | | 700 [°C] | | |
|---|---|---|---|---|---|---|---|---|---|---|---|---|---|---|---|
| Sample | $T_{50i}$ | $T_{50d}$ | ($T_H$ | $T_{50i}$ | $T_{50d}$ | ($T_H$ | $T_{50i}$ | $T_{50d}$ | ($T_H$ | $T_{50i}$ | $T_{50d}$ | ($T_H$ | $T_{50i}$ | $T_{50d}$ | ($T_H$ |
| $SnO_2$(Cl) | 328 | 291 | +37 | 327 | 291 | +36 | 195 | 222 | −27 | 194 | 231 | −36 | 152 | 234 | −82 |
| $SnO_2$(Fl) | 327 | 293 | +34 | 323 | 287 | +36 | 216 | 283 | −67 | 193 | 254 | −61 | 140 | 235 | −95 |

[a] $T_{50i}$ and $T_{50d}$ denote the temperature of 50% CO conversion reached during an increase and decrease in the temperature [°C]. $\Delta T_H$ is the difference ($T_{50i} - -T_{50d}$). Refer to text for further details.

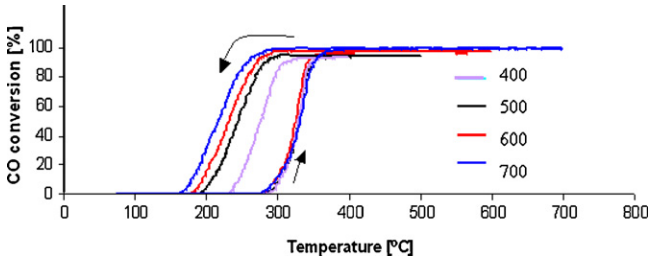


**Fig. 10.** CO conversion in the successive cycle of experiments at the temperature 400, 500, 600 and 700 °C, respectively.

was carried out and each subsequent experiment was finished at the temperature of about 100 °C higher than the previous one. The results are presented in Fig. 10. The most characteristic feature is the fact that in each case the reaction starts at practically the same temperature and that hysteresis gradually increases with the rise in the final temperature of the TPSR process. These results confirm the fact that the concentration of oxygen which shows higher reactivity increases with temperature although the total amount of oxygen adsorbed does not change.

The results of the catalytical activity presented up to now were obtained for the reacting mixture (0.35 vol.% CO, 99.65 vol.% air). If we double the concentration of CO in air (0.72 vol.% CO, 99.28 vol.% air), the shape of the curves illustrating the conversion of CO can change, which is presented in Fig. 11.

When the $SnO_2$(Fl) sample is pre-treated in oxygen at the temperatures lower than 500 °C, TPSR curves have a typical light-off shape identical to that presented in Fig. 7. For higher temperatures of pre-treating in oxygen, shapes of curves strongly change showing two temperature ranges of $SnO_2$ activity. The first one starts at ca. 85 °C, reaches its maximum between 135 and 150 °C, finishes at 160–180 °C and is followed by a typical light-off course; the second begins at ca. 270 °C. The low temperature activity is obviously connected with the removal of adsorbed oxygen. Such results are in accordance with the CO-TPR results presented earlier. CO consumption during TPR as well as TPSR in the first stage is similar. The above results confirm that the rate of oxygen readsorption is very low at temperatures characteristic of the first stage of TPSR. The correlation of TPR-CO and TPSR suggests that CO oxidation over $SnO_2$ and the reduction of $SnO_2$ may be described by the same mechanism.

## 4. Discussion

It is well known that the surface of tin dioxide in clean air or in the atmosphere containing oxygen may be covered by ionosorbed oxygen species [$O^-$] or [$O_2^-$], which are characterized by different chemical activity [29]. Literature date [19,30–33] also show that [$O^-$] species are more reactive than [$O_2^-$] and the dissociation of

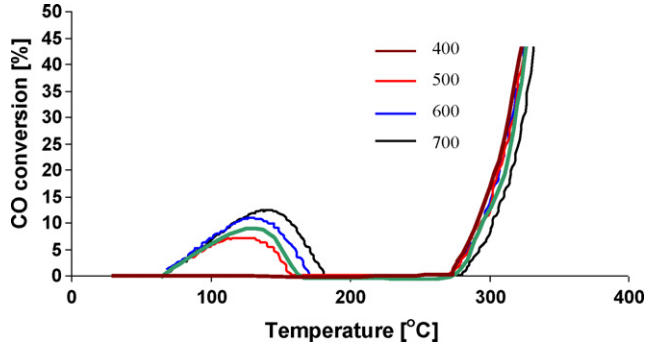


**Fig. 11.** CO conversion (reacting mixture: 0.72 vol.% CO, 99.28 vol.% air) vs. temperature for $SnO_2$(Fl) sample pre-treated in oxygen at different temperatures [°C].

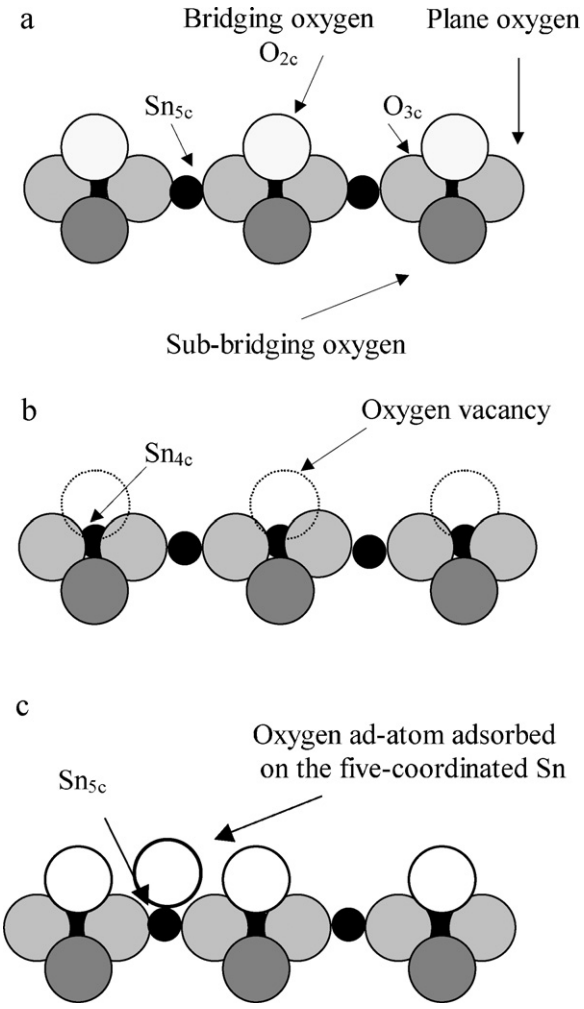


**Fig. 12.** The model of $SnO_2$ (1 1 0) surface: (a) – stoichiometric, (b) – reduced. Based on [36] (c) – "oxidised" with oxygen ad-atom.

[$O_2^-$] to [$O^-$] begins in the temperature range of 100–200 °C. Due to the presence of different reactive oxygen species and the fact that they appear at different temperatures during CO oxidation carried out by TPSR method, hysteresis can be observed. This hysteresis can be explained in terms of the type of oxygen species adsorbed on $SnO_2$ surface. When the TPSR process is carried out during the temperature increase, the adsorbed oxygen species can be either molecular ($O_2$) or ionic ($O_2^-$ and $O^-$). Oxygen species $O_2$ and $O_2^-$ are less reactive and are adsorbed at lower temperatures than $O^-$, which is adsorbed at a higher temperature and is the most reactive form of oxygen. Therefore when the TPSR measurement is taken at an increasing temperature, the less reactive oxygen species extract electrons from $SnO_2$ becoming gradually more reactive, and CO oxidation occurs. However, when the TPSR process is realised at a decreasing temperature, more reactive oxygen ions ($O^-$) remain adsorbed as the temperature is lowered. As a result, a higher conversion of CO is observed. The increase in the amounts of adsorbed $O^-$ species also leads to hysteresis.

TPD results show that oxygen adsorption practically does not occur at the temperature lower than 300 °C. It means that the concentration of oxygen species on the surface of $SnO_2$ samples is very low, especially that of the most reactive $O^-$. Thus, the reaction of CO oxidation does not occur according to the mechanism given above. However, the fact that CO conversion begins at the same temperature at which TPR process starts indicates that CO oxidation over $SnO_2$ may be described by Mars van Krevelen mechanism. Accord-

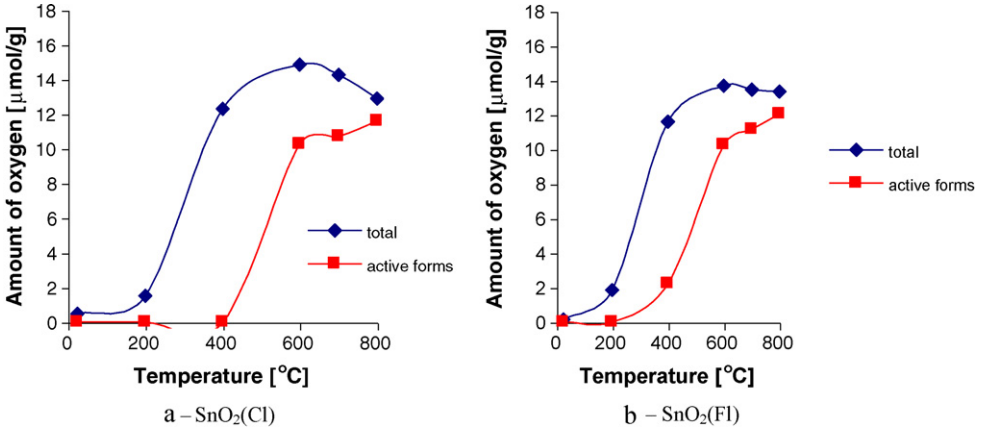


**Fig. 13.** The amount of total and active forms of $O_2$ vs. temperature of $O_2$ adsorption.

ing to this mechanism, oxidation of carbon monoxide precedes the reduction of an oxidised surface site, which is subsequently reoxidised by gas-phase molecular oxygen [34]. On the other hand, the detailed analysis and comparison of TPR and TPSR profiles show that Mars van Krevelen mechanism can be used to describe CO oxidation only in its initial stage. This conclusion results from the fact that at a given temperature CO conversion increases faster during TPSR than CO consumption during TPR. This enhancement of conversion may suggest that new catalytic centres are created.

We assume that such new catalytic centres are anion vacancies which arise on six coordinated tin cations. The structure of $SnO_2$ (1 1 0) surface, which is crucial for the following discussion, is shown in Fig. 12a and b. Tin dioxide (1 1 0) crystal face is the most stable [35] and, as it was earlier shown (Fig. 2), it is a major component of both $SnO_2$ samples investigated in this work.

Image of this surface was created on the basis of the work [36]. The stoichiometric (1 1 0) $SnO_2$ surface is depicted in Fig. 12a. According to work [37] the outmost atomic layer consists of two coordinated oxygen anions denoted as $O_{2c}$ and called bridging oxygen, which occupy the bridging position between six coordinated tin cations denoted as $Sn_{6c}$, located in the second layer. In this layer, there are also five coordinated tin cations $Sn_{5c}$ and three coordinated oxygen atoms $O_{3c}$.

The removal of the bridging oxygen layer from the stoichiometric surface leads to its reduction giving one bridging vacancy per unit cell and reduces the coordination of six coordinated tin atoms to four. These centres are denoted as $Sn_{4c}$. This kind of surface is called a reduced surface and it is shown in Fig. 12b.

During CO oxidation, when the temperature increases to that at which the reduction of $SnO_2$ starts, carbon monoxide reacts with atoms of bridging oxygen leading to the creation above mentioned vacancies. These vacancies are the centres for oxygen adsorption and are reoxidised by molecular oxygen from a gas phase. Basing on the literature data [38,39] and our results, one can postulate that the mechanism of reoxidation is connected with the dissociation of oxygen molecule. As a result, one oxygen atom fills anion vacancy, the second is adsorbed on the nearest five coordinated tin cation. Oxygen atom adsorbed on tin cation extracts electron from $SnO_2$ becoming the most reactive $O^-$ species. Such species lead to the enhancement of CO conversion and hysteresis phenomenon, described above. This mechanism can be expressed by the sequence of reactions

$$SnO_2 + CO = SnO + CO_2 \quad (6)$$

$$SnO + O_2 + e = SnO_2 \cdots O^- \quad (7)$$

$$SnO_2 \cdots O^- + CO = CO_2 + SnO_2 + e \quad (8)$$

Dissociation of oxygen may also take place on the reduced sample (Fig. 12b) when it is subjected to the treatment in oxygen at temperatures >500 °C. Also in this case one oxygen atom fills an oxygen vacancy, whereas the second one, called an ad-atom, adsorbed on $Sn_{5c}$ is able to create the reactive $O^-$ species. This process can be visualized by the scheme below:

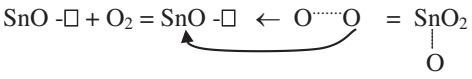


(9)

where □ is the anionic vacancy and SnO-□ the reduced surface of $SnO_2$.

As the result, "oxidised" surface shown in Fig. 12c is formed. The concentration of charged $O^-$ species should not exceed 1% of monolayer coverage, because of electrostatic reasons (Weisz limitation) [40].

The proposition that oxygen dissociates at bridging oxygen vacancies, filling the vacancy and producing an oxygen ad-atoms was postulated by authors of work [38]. The presence of these reactive oxygen ad-atoms is evident in the temperature-programmed reduction (Fig. 6). They are also accessible during CO oxidation leading to the significantly high catalytic activity of $SnO_2$ at low temperatures. However, this effect is not durable. Due to the depletion of highly active $O^-$ forms, this increased catalytic activity quickly lowers, especially at the higher concentration of carbon monoxide (Fig. 11). It also means that the rate of oxygen readsorption is so low that the reaction is limited by the concentration of adsorbed $O^-$ species. Thus taking the above into consideration one can assume that to get an effective $SnO_2$ catalyst for oxidation reactions, the promoters improving the ability of $SnO_2$ surface to oxygen readsorption should be applied.

In order to determine precisely the oxygen concentration which shows the highest reactivity, a pulse technique was used. The small volumes (0.05 $cm^3$) of hydrogen were introduced on the $SnO_2$ sample in the stream of carrier gas (argon 40 $cm^3$ $min^{-1}$). Prior to the reaction $SnO_2$ (0.2 g) was pre-treated in the stream of oxygen of high purity at different temperatures in the range 25–600 °C for 1 h. After cooling to room temperature, oxygen was changed to argon and the temperature was raised to 150 °C, at which the pulses of hydrogen were introduced on the $SnO_2$ sample. Temperature of 150 °C was chosen since according to the results presented earlier the maximum of low temperature CO conversion was recorded just at that temperature. This maximum is connected with reaction (9).

Fig. 13a and b shows the amount of the active forms of oxygen ($O^-$) species vs. temperature (red curves). These results are confronted with total oxygen adsorption obtained from TPD (blue curves). It can be observed that according to expectations the total

adsorption was in each case higher than adsorption of $O^-$. These differences are smaller for $SnO_2$(Fl) than for $SnO_2$(Cl), probably because of the presence of residual chlorine on the $SnO_2$ surface. Analysing these results one also can claim that in contrast to the total adsorption, adsorption of $O^-$ still increases with temperature. The difference between the total adsorption and adsorption of $O^-$ can be ascribed to oxygen which adsorbs on the $SnO_2$ surface without charge (weak adsorption).

The adsorption of $O_2$ on stoichiometric as well as on reduced (1 1 0) surface has been investigated based on theoretical methods [40]. Authors of work [41] state that weak adsorption is possible at the five coordinated $Sn_{5c}$ sites with an adsorption energy lower than 0. 4 eV. A much stronger adsorption is possible at bridging oxygen vacancy sites. There was also some evidence that a bridging oxygen vacancy can bind even three $O_2$ molecules simultaneously with one at the vacancy site and two at the nearest five coordinated $Sn_{5c}$ sites [42,43].

## 5. Conclusions

The main aim of this work was to determine if there is any relationship between adsorption of oxygen on $SnO_2$ and its activity in CO oxidation. The experimental results proved that such a relationship exists. Due to the presence of different reactive oxygen forms, CO oxidation shows the hysteretic course. The approach to the differentiated mechanism of CO oxidation over $SnO_2$ has been presented. The most surprising feature of CO oxidation over $SnO_2$ is its high (although short-lived) activity after pre-treatment in oxygen at temperatures higher than 500 °C. This phenomenon may be of significance for the explanation of mechanisms of gas detection on $SnO_2$ sensors.

## Acknowledgment

This work was supported by The Polish Scientific Research Council (KBN) Grant No. NN 209 180436.

## References

[1] S. Samson, C.G. Fonstad, J. Appl. Phys. 44 (1973) 4618.
[2] W. Gopel, Prog. Surf. Sci. 20 (1985) 9.
[3] W. Fliegel, G. Behr, J. Werner, G. Krabbes, Sens. Actuators B 18–19 (1994) 474.
[4] D.E. Williams, Sens. Actuators B 57 (1999) 1.
[5] N. Barsan, J.R. Stetter, M. Findlay, W. Gopel, Sens. Actuators B 66 (2000) 31.
[6] K. Sekizawa, H. Widjaja, S. Maeda, Y. Ozawa, K. Eguchi, Appl. Catal. A 200 (2000) 211.
[7] M. Watanabe, S. Venkatesan, H.A. Laitinen, J. Electrochem. Soc. 130 (1983) 59.
[8] R.E. Presley, C.L. Munsee, C.-H. Park, D. Hong, J.F. Wager, D.A. Keszler, J. Phys. D 37 (2004) 2810.
[9] T. Takeguchi, O. Takeoh, S. Aoyama, J. Ueda, R. Kikuchi, K. Eguchi, Appl. Catal. A 252 (2003) 205.
[10] P.G. Harrison, C. Bailey, W. Azelee, J. Catal. 186 (1999) 147.
[11] D.R. Schryer, B.T. Upchurch, B.D. Sidney, K.G. Brown, G.B. Hoflund, R.K. Herz, J. Catal. 130 (1991) 314.
[12] T. Matsui, T. Okanishi, K. Fujiwara, K. Tsutsui, R. Kikuchi, T. Takeguchi, K. Eguchi, Sci. Technol. Adv. Mater. 7 (2006) 524.
[13] K. Grass, H. Lintz, J. Catal. 172 (1997) 446.
[14] I. Kocemba, I. Chylak, J.M. Rynkowski, Przem. Chem. 85 (2006) 737.
[15] T. Kawabe, S. Shimomura, T. Karasuda, K. Tabata, E. Suzuki, Y. Yamaguchi, Surf. Sci. 448 (2000) 101.
[16] N. Barsan, M. Schweizer-Berberich, W. Göpel, Fresenius J. Anal. Chem. 365 (1999) 287.
[17] S.C. Chang, J. Vac. Sci. Technol. 17 (1980) 366.
[18] A. Bielański, J. Haber, Catal. Rev. Sci. Eng. 19 (1979) 1.
[19] M.M. Che, A.J. Tench, Adv. Catal. 31 (1982) 77;
M.M. Che, A.J. Tench, Adv. Catal. 32 (1983) 1.
[20] L. Bruno, C. Pijolat, R. Lalauze, Sens. Actuators B 18–19 (1994) 195.
[21] L.I. Poopova, M.G. Michailov, V.K. Gueorguiev, Thin Solid Films 186 (1990) 107.
[22] M. Ivanovskaya, J. Electron. Technol. 33 (2000) 108.
[23] J.F. McAleer, P.T. Moseley, J.O.W. Norris, D.E. Williams, J. Chem. Soc. Faraday Trans. 83 (1987) 1323.
[24] I. Kocemba, Przem. Chem. 82 (2003) 142.
[25] H.P. Klug, L.E. Alexander, X-Ray Diffraction Procedures, Wiley, New York, 1967.
[26] S. Saukko, Ulla Lassi, V. Lanttoa, M. Kroneld, S. Novikov, P. Kuivalainen, T. Rantala, J. Mizsei, Thin Solid Films 490 (2005) 48.
[27] F. Gaillard, M. Abdat, J.P. Joly, A. Perrard, Appl. Surf. Sci. 238 (2004) 91.
[28] N. Yamazoe, J. Fuchigami, M. Kishikawa, T. Seiyama, Surf. Sci. 86 (1979) 335.
[29] B. Kamp, R. Merkle, R. Lauck, J. Maier, J. Solid State Chem. 178 (2005) 3027.
[30] G. Sberveglieri, G. Coccoli, P. Benussi, S. Groppelli, P. Nelli, Appl. Surf. Sci. 40 (1989) 169.
[31] W. Gopel, G. Rocker, R. Feierabend, Phys. Rev. B 28 (1983) 3427.
[32] C. Canevali, N. Chiodini, P. Di Nola, F. Morazzoni, R. Scottia, C.L. Bianchib, J. Mater. Chem. 7 (1997) 997.
[33] M.A. Maki-Jaskari, T.T. Rantala, V.V. Golovanov, Surf. Sci. 577 (2005) 127.
[34] P. Mars, D.W. van Krevelen, Spec. Suppl. Chem. Eng. Sci. 3 (1954) 41.
[35] V.E. Henrich, P.A. Cox, The Surface Science of Metal Oxides, Cambridge University Press, Cambridge, 1994.
[36] M. Habgood, N. Harrison, Surf. Sci. 602 (2008) 1072.
[37] F.R. Sensato, R. Custódio, M. Calatayund, A. Beltran, J. Andrés, J.R. Sambrano, E. Longo, Surf. Sci. 511 (2002) 408.
[38] B. Slater, C.R.A. Catlow, D.E. Williams, A.M. Stoneham, Chem. Commun. 0 (2000) 1235.
[39] W.S. Epling, Ch. Peden, M. Henderson, U. Diebold, Surf. Sci. 412/413 (1998) 333.
[40] P.B. Weisz, J. Chem. Phys. 21 (1953) 1531.
[41] A. Maiti, J.A. Rodriguez, M. Law, P. Kung, J.R. McKinney, P. Yang, Nano Lett. 3 (2003) 1025.
[42] J. Oviedo, M.J. Gillan, Surf. Sci. 490 (2001) 221.
[43] M. Batzill, U. Diebold, Prog. Surf. Sci. 79 (2005) 47.